

Effective-Range Expansion of the Neutron-Deuteron Scattering Studied by a Quark-Model Nonlocal Gaussian Potential

Kenji FUKUKAWA and Yoshikazu FUJIWARA

Department of Physics, Kyoto University, Kyoto 606-8502, Japan

The S -wave effective range parameters of the neutron-deuteron (nd) scattering are derived in the Faddeev formalism, using a nonlocal Gaussian potential based on the quark-model baryon-baryon interaction fss2. The spin-doublet low-energy eigenphase shift is sufficiently attractive to reproduce predictions by the AV18 plus Urbana three-nucleon force, yielding the observed value of the scattering length $^2a_{nd}$ and the correct differential cross sections below the deuteron breakup threshold. This conclusion is consistent with the previous result for the triton binding energy, which is nearly reproduced by fss2 without reinforcing it with the three-nucleon force.

Subject Index: 205

§1. Introduction

Few-nucleon systems are best suited to study the underlying nucleon-nucleon (NN) interaction and its extension to few-nucleon forces, since many sophisticated techniques to solve the systems yield equivalent results that can be compared with ample experimental data.^{1),2)} In fact, the three-nucleon ($3N$) system is already solved with many realistic meson-exchange potentials, yielding insufficient binding energies of the triton missing 0.5 to 1 MeV without the $3N$ force.³⁾ An attempt to reproduce the NN and $3N$ data consistently is pursued by using the chiral effective field theory, but a complete reproduction of all the $3N$ data in this approach is still beyond away.^{4),5)} We have applied the quark-model (QM) baryon-baryon (BB) interaction^{6),7)} to the triton and hypertriton in the Faddeev formalism and obtained many interesting results.⁸⁾⁻¹¹⁾ The most recent model fss2 gives a nearly correct binding energy of the triton with the correct root-mean-square radius, preserving the sufficient strength of the tensor force for the deuteron and the correct 1S_0 NN scattering length.⁸⁾ This result indicates that fss2 is sufficiently attractive in the $^2S_{1/2}$ channel of the $3N$ system without the $3N$ force. In this channel, the deuteron distortion effect related to the strong short-range repulsion of the NN interaction is very important. In the QM BB interaction, this part is mainly described by the quark-exchange nonlocal kernel of the one-gluon exchange Fermi-Breit interaction, which has quite different off-shell properties from the phenomenological repulsive core described by local potentials in the standard meson-exchange models. The nonlocal effect resulting from the exact antisymmetrization of six quarks is very important to reproduce the nearly correct triton binding energy.

The QM BB interaction is constructed for two three-quark clusters in the framework of the resonating-group method (RGM). It is characterized not only by the dominant nonlocality from the interaction kernel, but also by the energy dependence originating from the normalization kernel. In the original evaluation of the triton and

hypertriton binding energies, this energy dependence is determined self-consistently by calculating the expectation value of the two-cluster Hamiltonian with the square integrable three-cluster wave function.⁸⁾⁻¹⁰⁾ This prescription is however not applicable to the scattering problem, since the scattering wave function is not square integrable. In the final form of the triton and hypertriton Faddeev calculations,¹¹⁾ the energy dependence of the RGM kernel is eliminated by a standard off-shell transformation, using the square root of the normalization kernel.¹²⁾ An extra nonlocality emerges from this off-shell transformation as a result of eliminating the energy dependence of the RGM kernel. It is shown in Ref.11) that this renormalized RGM prescription gives a slightly less attractive effect to the triton and hypertriton binding energies, in comparison with the previous self-consistent treatment. The 350 keV deficiency of the triton binding energy predicted by fss2 after the charge dependence correction of the NN interaction is still much smaller than 0.5 to 1 MeV given by the standard meson-exchange potentials. It is therefore interesting to examine the nonlocal effect of the QM NN interaction to the $3N$ scattering observables, such as the scattering lengths, the differential cross sections and the spin polarization, in this energy-independent QM NN interaction.

The numerical calculation of the three-body scattering using the QM BB interaction is very time consuming due to the complex structure of the interaction. We therefore construct a nonlocal Gaussian potential in the isospin basis by applying the Gauss-Legendre integration formula to special functions appearing in the exchange RGM kernel.¹³⁾ The nonlocality and the energy dependence of the QM BB interaction is strictly preserved in the nonlocal Gaussian potential. We find that the 15-point Gauss-Legendre integration formula is good enough to carry out the few-body calculations accurately. The NN phase shifts predicted by this potential are essentially the same as those by fss2 with accuracy of less than 0.1° . We will show that the difference in the triton binding energy between fss2 and this nonlocal Gaussian potential is only 15 keV.

Here, we study the low-energy neutron-deuteron (nd) elastic scattering below the deuteron breakup threshold based on the formulation developed in Ref.14). For this purpose, the S -wave effective range theory in the channel-spin formalism is very useful. The channel spin S_c is composed of the NN total angular momentum I and the spin $1/2$ of the third nucleon.¹⁵⁾ Since the deuteron channel with $I = 1$ only survives in the asymptotic region, the scattering amplitudes for the nd elastic scattering are specified by the channel spin $S_c = 1/2$ (the spin-doublet channel) and $S_c = 3/2$ (the spin-quartet channel). These two channels have quite different characteristics with respect to the deuteron distortion effect. Namely, in the spin-quartet channel the incident neutron can not penetrate deep inside of the deuteron due to the effect of the Pauli principle, resulting in the weak distortion effect of the deuteron. On the other hand, the neutron can freely approach to the deuteron in the spin-doublet channel, causing strong distortion effects reflecting strong sensitivity to details of the NN interaction. In this sense, the spin-doublet scattering length $^2a_{nd}$ becomes an important observable to measure if the NN interaction is appropriate or not. It is known for a long time that a larger triton binding energy corresponds to a smaller $^2a_{nd}$. This linear correlation is known as the Phillips line,¹⁶⁾ and is

confirmed by many theoretical calculations.^{17)–24)} Since the binding energy of the triton is not reproduced in the NN meson-exchange potentials, the experimental value, ${}^2a_{nd} = 0.65 \pm 0.04$ fm,²⁵⁾ is not reproduced either. The calculated ${}^2a_{nd}$ is more than 0.9 fm if only an NN force is used. It is therefore a common practice to add the $3N$ force to reproduce the triton binding energy as well as the correct ${}^2a_{nd}$. A thorough investigation of the triton binding energy and the scattering lengths, using a number of meson-exchange potentials and various $3N$ forces, is given in Ref. 23). We can expect that the nonlocal effect of fss2 leads to a good reproduction of the doublet scattering length since fss2 gives a large triton binding energy close to the experiment. In Ref. 24), an application of the nonlocal interaction to the nd scattering lengths was made, using the NN interaction based on the chiral constituent quark model.^{26),27)} Since their Faddeev calculation does not treat the energy dependence of the QM NN interaction properly, they have obtained an insufficient triton binding energy²⁸⁾ and a large doublet scattering length ${}^2a_{nd}$,²⁴⁾ almost comparable to the meson-exchange predictions.

The most accurate method to determine the scattering lengths is to calculate the zero-energy scattering amplitude directly, as carried out in Refs. 17), 18), 23), 24), etc. In this approach, however, the zero-energy nd scattering is only examined. More extensive study of the low-energy nd elastic scattering can be achieved in terms of the effective range theory,^{16),19)} in which a pole structure existing in the effective-range function for the doublet- S channel should be properly taken into account.^{29)–32)} We can discuss the energy dependence of the low-energy S -wave phase shifts in this approach. On the other hand, this method has a problem of numerical inaccuracy at extremely low energies below 100 keV in the center-of-mass (cm) system, since the solution of the basic equation becomes very singular in the momentum representation.

In this paper, we start with the nonlocal Gaussian QM NN interaction and eliminate the energy dependence numerically in the above mentioned renormalized RGM formalism. We then apply this interaction to the nd scattering and solve the Alt-Grassberger-Sahndhas (AGS) equation³³⁾ to obtain the scattering amplitudes. The elastic scattering amplitudes are conveniently parameterized by the standard eigenphase shifts and mixing parameters defined in Ref. 15). The spin-doublet and quartet S -wave effective range parameters: i.e., ${}^2a_{nd}$, $({}^2r_e)_{nd}$, ${}^4a_{nd}$ and $({}^4r_e)_{nd}$, together with the pole parameter q_Q in the doublet case, are calculated by employing the S -wave single-channel effective range formula. We find reasonable agreement of the low-energy differential cross sections with the nd experimental data. Since the nd data have rather large error bars, we will also evaluate the differential cross sections of the pd elastic scattering by employing a simple prescription, called the Coulomb externally corrected approximation,^{34),35)} to incorporate the Coulomb effect with some modifications to the nuclear phase shifts. We will find that the ${}^2S_{1/2}$ eigenphase shift predicted by our model is sufficiently attractive to reproduce the doublet scattering length ${}^2a_{nd}$ and the low-energy nd and pd differential cross sections. It is possible that the correct treatment of the Coulomb effect can reproduce the pd differential cross sections and the polarization observables below the deuteron breakup threshold without introducing the $3N$ force.

The organization of this paper is as follows. In §2.1, a brief description of the Faddeev formalism is given for the bound-state and nd scattering problems. The spin-isospin factors and rearrangement factors for the permutation operator are explicitly given in Appendix A. In §2.2, we recapitulate the procedure to obtain the eigenphase shifts and their J -averaged central phase shifts from the solutions of the AGS equation. The single-channel effective-range expansion is explained in §2.3. The eigenphase shifts of our model are compared in §3.1 with those of Argonne V18 (AV18) plus Urbana $3N$ force, obtained by the K -harmonics technique. The nd and pd differential cross sections below the deuteron breakup threshold are also discussed. The effective range parameters are given in §3.2, together with the analysis of the S -wave contributions to the nd total cross sections. The last section is devoted to a summary.

§2. Formulation

2.1. Faddeev approach to the triton and the nd scattering

We start with the three-body Schrödinger equation

$$[E - H_0 - V_\alpha^{\text{RGM}} - V_\beta^{\text{RGM}} - V_\gamma^{\text{RGM}}]\Psi = 0, \quad (2.1)$$

where V_α^{RGM} denotes the energy-independent renormalized RGM kernel for which the detailed derivation is given in Ref. 14). The subscripts α , β and γ in Eq. (2.1) specify the types of Jacobi coordinates related to the residual pair in the usual way, with (α, β, γ) being the cyclic permutation of (123). For the systems of three identical particles, the Faddeev equation for the bound state reads

$$\psi = G_0 t P \psi, \quad (2.2)$$

where $P = P_{(12)}P_{(13)} + P_{(13)}P_{(12)}$ is a sum of the permutation operators for the nucleon rearrangement.³⁶⁾ The NN t -matrix in the three-body model space is derived from the standard Lippmann-Schwinger equation $t = v + vG_0t$ with $v = V^{\text{RGM}}$, where $G_0 = 1/(E - H_0)$ is the three-body Green function for the free motion. It is composed of the negative total energy E in the cm system and the three-body kinetic-energy operator $H_0 = h_0 + \bar{h}_0$. The operators h_0 and \bar{h}_0 correspond to the kinetic energy for $\mathbf{p}_3 = (1/2)(\mathbf{k}_1 - \mathbf{k}_2)$ and $\mathbf{q}_3 = (1/3)(2\mathbf{k}_3 - (\mathbf{k}_1 + \mathbf{k}_2))$ respectively when the Jacobi coordinates with $\gamma = 3$ is chosen. The vector \mathbf{k}_i is the individual momentum of particle i . The Faddeev component ψ is defined through $\psi = G_0 v \Psi$, with the total wave function $\Psi = \sum_\alpha \psi_\alpha$ in Eq. (2.1). In the partial wave expansion, we use the channel-spin formalism specified by $(I\frac{1}{2})S_c$. The relative angular momentum ℓ between the spectator nucleon and the NN subsystem is coupled with channel spin S_c and makes the total angular momentum $(\ell S_c)J$. The NN channel is specified by $(\lambda s)I; t$, where λ , s and t are the orbital angular momentum, the spin and the isospin of the NN system, respectively. The NN isospin t is uniquely specified by λ and s from the Pauli principle $(-)^{\lambda+s+t} = -1$. We further set the parity restriction $\pi = (-)^{\lambda+\ell}$, which is conserved for each J . The angular-spin-isospin wave functions

are thus defined by

$$\begin{aligned} |\mathbf{p}, \mathbf{q}; 123\rangle &= \sum_{\gamma} |p, q, \gamma\rangle \langle \gamma | \widehat{\mathbf{p}}, \widehat{\mathbf{q}}; 123\rangle, \\ \langle \widehat{\mathbf{p}}, \widehat{\mathbf{q}}; 123 | \gamma \rangle &= [Y_{\ell}(\widehat{\mathbf{q}}) [[Y_{\lambda}(\widehat{\mathbf{p}}) \chi_{st}(1, 2)]_I \chi_{\frac{1}{2}\frac{1}{2}}(3)]_{S_c}]_{JJ_z; \frac{1}{2}T_z}, \end{aligned} \quad (2.3)$$

with $\gamma = [\ell[(\lambda s)I_{\frac{1}{2}}]S_c]JJ_z; (t_{\frac{1}{2}})_{\frac{1}{2}}T_z$ in the channel-spin representation. The partial wave expansion of the Faddeev equation in Eq. (2.2) is given by

$$\begin{aligned} \psi_{\gamma}(p, q) &= -\frac{M}{\hbar^2} \frac{1}{\kappa_t^2 + p^2 + (3/4)q^2} \sum_{\gamma', \gamma''} \int_0^{\infty} dq' q'^2 \int_0^{\infty} dp' p'^2 \int_0^{\infty} dq'' q''^2 \\ &\times \int_0^{\infty} dp'' p''^2 \langle p, q, \gamma | t | p', q', \gamma' \rangle \langle p', q', \gamma' | P | p'', q'', \gamma'' \rangle \psi_{\gamma''}(p'', q''), \end{aligned} \quad (2.4)$$

where $M = (M_n + M_p)/2$ is the averaged nucleon mass in the isospin formalism. The binding energy of the triton is deduced from $E_B = (-E) = (\hbar^2/M)\kappa_t^2$. The coupled integral equation for p and q in Eq. (2.4) is solved in the Lanczos-Arnoldi method after the necessary process of discretization. See Ref. 8) for details. The NN t -matrix is factorized as

$$\langle p, q, \gamma | t | p', q', \gamma' \rangle = \frac{4\pi}{(2\pi)^3} \frac{\delta(q - q')}{qq'} t_{\gamma\gamma'} \left(p, p'; E - \frac{3\hbar^2}{4M} q'^2 \right). \quad (2.5)$$

The matrix element of the permutation operator is evaluated as

$$\langle p, q, \gamma | P | p', q', \gamma' \rangle = \frac{1}{2} \int_{-1}^1 dx \frac{\delta(p - p_1)}{p^{\lambda+2}} g_{\gamma, \gamma'}(q, q', x) \frac{\delta(p' - p_2)}{p'^{\lambda'+2}}, \quad (2.6)$$

with $p_1 = p(q', q/2; x)$, $p_2 = p(q, q'/2; x)$ and $p(a, b; x) = \sqrt{a^2 + b^2 + 2abx}$. The basic rearrangement coefficients $g_{\gamma, \gamma'}(q, q', x)$ contain the spin-isospin factors and the explicit expression depends on a specific type of the channel-coupling scheme, as given in Appendix A.

For the nd scattering, the three-body scattering amplitudes are obtained by solving the AGS equation³⁷⁾

$$U|\phi\rangle = G_0^{-1}P|\phi\rangle + PtG_0U|\phi\rangle, \quad (2.7)$$

where $|\phi\rangle = |\mathbf{q}_0, \psi_d\rangle$ is the plane-wave channel wave function with $|\psi_d\rangle$ being the deuteron wave function. The total cm energy E in $G_0^{-1} = E + i0 - H_0$ is expressed as $E = E_{\text{cm}} + \varepsilon_d$, where $E_{\text{cm}} = (3\hbar^2/4M)q_0^2$ is the cm incident energy of the neutron and $|\varepsilon_d| = -\varepsilon_d$ is the deuteron binding energy. In the AGS equation, we have in general two types of singularities, but the notorious moving singularity does not appear for the energies below the deuteron breakup threshold. The other singularity related to the deuteron pole of the NN t -matrix is directly incorporated to the AGS equation in the Noyes-Kowalski method. For the detailed procedure to overcome difficulties of these singularities, Ref. 14) should be referred to. Here, we recapitulate

the method to derive the elastic scattering amplitudes. The singularity of the NN t -matrix is separated as

$$t = \tilde{t} - icG_0^{-1}|\phi\rangle\langle\phi|G_0^{-1} \quad \text{with} \quad c = 2\pi\frac{q_0M}{3\hbar^2}. \quad (2.8)$$

If we use the principal-value t -matrix \tilde{t} in Eq. (2.7), we obtain

$$U|\phi\rangle = G_0^{-1}P|\phi\rangle[1 - ic\langle\phi|U|\phi\rangle] + P\tilde{t}G_0U|\phi\rangle. \quad (2.9)$$

We eliminate the first term of Eq. (2.9) by defining W as

$$W = G_0P - P|\phi\rangle Z^{-1}\langle\phi|P \quad \text{with} \quad Z = \langle\phi|G_0^{-1}P|\phi\rangle. \quad (2.10)$$

Our basic equation is

$$\tilde{Q}|\phi\rangle = \tilde{P}|\phi\rangle + W\tilde{t}\tilde{Q}|\phi\rangle, \quad (2.11)$$

where $\tilde{Q}|\phi\rangle$ and $\tilde{P}|\phi\rangle$ is defined through

$$G_0U|\phi\rangle = \tilde{Q}|\phi\rangle\langle\phi|U|\phi\rangle, \quad \tilde{P}|\phi\rangle = P|\phi\rangle Z^{-1}. \quad (2.12)$$

The elastic scattering amplitudes are obtained by multiplying Eq. (2.9) with $Z^{-1}\langle\phi|$ from the left-hand side. One can easily show

$$\langle\phi|U|\phi\rangle = [Z^{-1} - \langle\phi|X|\phi\rangle + ic]^{-1} \quad \text{with} \quad \langle\phi|X|\phi\rangle = \langle\phi|\tilde{P}\tilde{t}\tilde{Q}|\phi\rangle. \quad (2.13)$$

The partial wave components of the scattering amplitude, $U_{(\ell'S'_c),(\ell S_c)}^J = \langle\phi_{\ell'S'_c}|U|\phi_{\ell S_c}\rangle$, are defined by

$$\begin{aligned} \langle\phi_{\mathbf{q}_f}; S'_c S'_{cz}|U|\phi_{\mathbf{q}_i}; S_c S_{cz}\rangle &= \sum_{\ell' \ell J J_z} U_{(\ell'S'_c),(\ell S_c)}^J \\ &\times \sum_{m'} \langle\ell' m' S'_c S'_{cz}|J J_z\rangle Y_{\ell' m'}(\hat{\mathbf{q}}_f) \sum_m \langle\ell m S_c S_{cz}|J J_z\rangle Y_{\ell m}^*(\hat{\mathbf{q}}_i), \end{aligned} \quad (2.14)$$

with $|\mathbf{q}_f| = |\mathbf{q}_i| = q_0$. Once the partial wave components of $\langle\phi|X|\phi\rangle$ is calculated, $U_{(\ell'S'_c),(\ell S_c)}^J$ is obtained by solving an equation,

$$\sum_{\ell', S'_c} [(Z^{-1})_{\ell S_c, \ell' S'_c} - X_{\ell S_c, \ell' S'_c} + ic \delta_{\ell, \ell'} \delta_{S_c, S'_c}] U_{(\ell' S'_c), (\ell S_c)}^J = \delta_{\ell, \ell'} \delta_{S_c, S'_c}. \quad (2.15)$$

The coupled channel S -matrix is given by $S_{(\ell S_c), (\ell' S'_c)}^J = \delta_{\ell, \ell'} \delta_{S_c, S'_c} - 2ic U_{(\ell S_c), (\ell' S'_c)}^J$.

2.2. Eigenphase shifts

In the channel-spin representation, the asymptotic channel wave function $|\phi; (\ell S_c) J J_z\rangle$ in the partial wave expansion is specified by $(\ell S_c) J = (J \pm 3/2, 3/2) J$, $(J \mp 1/2, 1/2) J$, and $(J \mp 1/2, 3/2) J$ for the parity $\pi = (-)^{J \mp 1/2}$. Therefore, the S -matrix $S_{(\ell S_c), (\ell' S'_c)}^J$ is a two-dimensional matrix for $J = 1/2$, and a three-dimensional matrix for $J \neq 1/2$. The S -matrix can be diagonalized as

$$S = U^\dagger e^{2i\Delta} U, \quad (2.16)$$

where Δ is the diagonal matrix of the eigenphase shifts $\delta_{\ell S_c}^J$. (We follow the notation in Ref. 15), but we should note that ℓ and S_c are not good quantum numbers.) The matrix U can be parameterized in terms of the mixing parameters ε, ξ and η ,¹⁵⁾

$$\begin{aligned}
 U &= \begin{pmatrix} 1 & 0 & 0 \\ 0 & \cos \varepsilon & \sin \varepsilon \\ 0 & -\sin \varepsilon & \cos \varepsilon \end{pmatrix} \begin{pmatrix} \cos \xi & 0 & \sin \xi \\ 0 & 1 & 0 \\ -\sin \xi & 0 & \cos \xi \end{pmatrix} \begin{pmatrix} \cos \eta & \sin \eta & 0 \\ -\sin \eta & \cos \eta & 0 \\ 0 & 0 & 1 \end{pmatrix} \\
 &= \begin{pmatrix} \cos \xi \cos \eta & \cos \xi \sin \eta & \sin \xi \\ -\cos \varepsilon \sin \eta - \sin \varepsilon \sin \xi \cos \eta & \cos \varepsilon \cos \eta - \sin \varepsilon \sin \xi \sin \eta & \sin \varepsilon \cos \xi \\ \sin \varepsilon \sin \eta - \cos \varepsilon \sin \xi \cos \eta & -\sin \varepsilon \cos \eta - \cos \varepsilon \sin \xi \sin \eta & \cos \varepsilon \cos \xi \end{pmatrix}.
 \end{aligned} \tag{2.17}$$

We assume $\varepsilon = \xi = 0$ for the $J^\pi = 1/2^+$ and $\xi = \eta = 0$ for the $J^\pi = 1/2^-$. By using a function,

$$\text{Arctan } z = \frac{1}{2i} \text{Log} \frac{1+iz}{1-iz}, \tag{2.18}$$

we can calculate the mixing parameters ε, ξ and η from the following equations:

$$\begin{aligned}
 \eta &= \text{Arctan} \frac{U_{12}}{U_{11}}, \quad \xi = -\text{Arctan} \left(\frac{U_{31} \cos \eta + U_{32} \sin \eta}{U_{33}} \right), \\
 \varepsilon &= -\text{Arctan} \left(\frac{U_{31} \sin \eta - U_{32} \cos \eta}{U_{21} \sin \eta - U_{22} \cos \eta} \right),
 \end{aligned} \tag{2.19}$$

where U_{ij} is the (i, j) component of the matrix U .

Before applying Eq. (2.19), we should reorder the eigenstates of Eq. (2.16) such that the leading term of the eigenvectors follows the decreasing order. This prescription corresponds to the rule to assign the eigenphases to such quantum numbers as having the dominant components of the eigenvectors.*) For energies above the breakup threshold, all the angles become complex. The largest component of the eigenvector is given by a real positive number. This gives an ambiguity of the sign of the mixing angles, which in turn comes from the phase convention of the eigenstates. We should note that Eq. (2.19) is most convenient if the diagonal U_{ii} components are close to one. This is because the mixing angles are usually very small with the magnitude of several degrees (except for $E_{\text{cm}} > \text{a few MeV}$ in the ${}^2P_{J-4}P_J$ couplings).

Since the difference in the eigenphase shifts with the same (ℓS_c) but different J is very small, the J -averaged central phase shift $\delta_{\ell S_c}^C$ is convenient to discuss the scattering cross sections approximately. The J -averaged central phase shift is defined by taking an average of all possible J states ${}^{2S_c+1}\ell_J$ with the weight factor $(2J+1)$,

$$\delta_{\ell S_c}^C = \frac{1}{(2\ell+1)(2S_c+1)} \sum_J (2J+1) \delta_{\ell S_c}^J. \tag{2.20}$$

The differential cross section for the nd elastic scattering is calculated by summing over the final spin states and by taking an average over the initial spin states. This

*) This rule is not applied to the case of ${}^2P_{3/2-4}P_{3/2}$ coupling for $E_{\text{cm}} > 40$ MeV, where the magnitude of the mixing parameter ε exceeds 45° .

is given by

$$\frac{d\sigma}{d\Omega} = \frac{1}{3} \left(\frac{d\sigma}{d\Omega} \right)^{S_c=1/2} + \frac{2}{3} \left(\frac{d\sigma}{d\Omega} \right)^{S_c=3/2}, \quad (2.21)$$

where the differential cross section for each channel spin S_c is calculated from the scattering amplitudes $f_\ell = (1/q_0)e^{i\delta_\ell} \sin \delta_\ell$ through

$$\left(\frac{d\sigma}{d\Omega} \right)^{S_c} = \left| \sum_{\ell} (2\ell + 1) f_\ell P_\ell(\cos \theta) \right|^2. \quad (2.22)$$

Here, we abbreviate the J -averaged central phase shift $\delta_{\ell S_c}^C$ to δ_ℓ for each S_c . In order to compare our results with the experimental data, we have to take into account the Coulomb force for the pd scattering. The comparison with the pd data is desirable since they are abundant and more accurate than those of the nd scattering. For example, in Refs. 38)–43) many phase shift analyses have been carried out with high accuracy. The exact treatment of the Coulomb force in the three-body problem is still a challenging task.^{34),35),44),45)} Because of its long-range nature, the Coulomb potential is not amenable to the standard scattering theory. We therefore incorporate the Coulomb effect to evaluate the differential cross sections of the pd elastic scattering, by employing a following simple prescription with some modifications to the nuclear phase shifts. The single channel differential cross section is given by,

$$\left(\frac{d\sigma}{d\Omega} \right)^{S_c} = \left| e^{-2i\sigma_0} f^C(\theta) + \sum_{\ell} (2\ell + 1) e^{2i(\sigma_\ell - \sigma_0)} f_\ell^N P_\ell(\cos \theta) \right|^2, \quad (2.23)$$

where $f^C(\theta)$ is the standard Coulomb scattering amplitude. The scattering amplitude from the strong interaction, f_ℓ^N in Eq. (2.23), is estimated from the nd eigenphase shifts of fss2 by adding the difference of the corresponding quantities for the pd and nd scattering, which will be taken from published results for other NN interactions. In Eq. (2.23), the partial-wave Coulomb phase shift σ_ℓ is given by $\sigma_\ell = \arg \Gamma(\ell + 1 + i\eta)$ with the Sommerfeld parameter η for the relative motion of the proton and the deuteron.

2.3. Effective-range expansion for the nd scattering

If we use the effective range theory, we can study energy dependence of the phase shifts reflected in the effective range r_e and discuss contributions to the total cross sections from the S -wave components between the neutron and the deuteron. We first calculate the eigenphase shifts for $J^\pi = 1/2^+$ and $3/2^+$ states. In the case of $J^\pi = 1/2^+$, the ${}^2S_{1/2}$ and ${}^4D_{1/2}$ channels are coupled. For the neutron energies below the deuteron breakup threshold, the phase shifts and mixing parameters are small except for the dominant S -wave eigenphase shift, so that the effective-range expansion formula for a single channel problem can be safely applied to this component to obtain the effective range parameters. This is also the case for the $J^\pi = 3/2^+$ state, where the ${}^4S_{3/2}$, ${}^2D_{3/2}$ and ${}^4D_{3/2}$ channels are coupled. In the quartet S -channel,

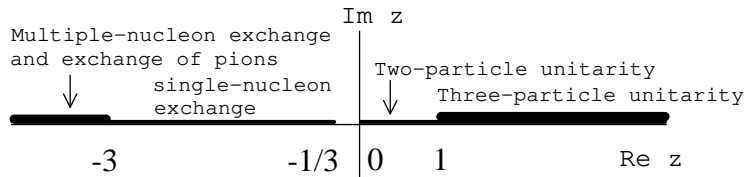


Fig. 1. The cut structure used in the N/D formalism for the nd elastic scattering amplitude in the complex z plane.³²⁾ Here, z is defined by $z = E_{\text{cm}}/|\varepsilon_d|$.

we can expand the effective-range function $K(q_0) = q_0 \cot \delta$ in the power series of q_0^2 :

$$K(q_0) = -\frac{1}{a} + \frac{1}{2}r_e q_0^2 + \mathcal{O}(q_0^4), \quad (2.24)$$

where a is the scattering length, r_e is the effective range, and $\delta = \delta_{0\frac{3}{2}}^{\frac{3}{2}}$ in $K(q_0) = q_0 \cot \delta$ is the S -wave eigenphase shift for the quartet channel with q_0 being the relative wave number between the neutron and the deuteron.

In the doublet- S channel, the effective-range function $K(q_0)$, which is the real part of the inverse scattering amplitude, has a pole just below the elastic threshold.^{29)–32)} We parameterize the effective-range function in the doublet channel as

$$K(q_0) = \frac{-\frac{1}{a} + \frac{1}{2}r_e q_0^2 + \mathcal{O}(q_0^4)}{1 + (q_0/q_Q)^2}, \quad (2.25)$$

where a pole parameter q_Q specifies the pole position, and $\delta = \delta_{0\frac{1}{2}}^{\frac{1}{2}}$ is the S -wave eigenphase shift for the doublet channel. The origin of this pole structure is studied by means of N/D equations.^{30)–32)} In the N/D formalism, the partial wave components of the scattering amplitude are given by $N(z)/D(z)$, where $N(z)$ and $D(z)$ are the analytic functions of the complex and dimensionless energy variable z defined by $z = E_{\text{cm}}/|\varepsilon_d|$. The two and three-body unitarities and the cut structure in the negative energy, which are shown in Fig. 1, yield the relationship, $N(z) = -z^{-\frac{1}{2}}\text{Im } D(z)$. The N/D equations are usually constructed by applying the Kramers-Kronig relations to $N(z)$ and $D(z)$. From the solution of the N/D equation, it was found that this singularity are brought about by both the dominant single-nucleon exchange and the other effects such as the two-nucleon exchange etc. slowly varying for small z . In the doublet channel, the single-nucleon exchange, which is by far the longest-range force, is attractive. Thus, nothing prevents the other effects from influencing the low-energy scattering. On the other hand, the single-nucleon exchange is strongly repulsive in the quartet channel. Therefore, the nucleons in this channel can not penetrate to the region where the other attractive forces could act. This is why the pole structure is found only in the doublet channel.

§3. Results and Discussion

3.1. Eigenphase shifts

The direct comparison of the nd eigenphase shifts, predicted by fss2, with the results of the modern phase shift analysis for the pd scattering is not possible because of the Coulomb effect. We therefore list in Table I our results for the energies of $E_n=1, 2$ and 3 MeV together with other theoretical predictions by the Pisa group,⁴²⁾ which are calculated using Argonne V18 NN potential (AV18)⁴⁶⁾ and AV18+Urbana(UR) $3N$ potentials.⁴⁷⁾ Here, $E_n = (3/2)E_{\text{cm}}$ is the neutron incident energy measured in the laboratory system. We have included the NN interaction up to the total angular momentum $I_{\text{max}}=4$ and the momentum mesh points $n \equiv n_1-n_2-n_3 = 12-6-5$ in the notation defined in §3.1 of Ref. 14). The UR $3N$ potential gives a sizable effect of about three to four degrees only on the $J^\pi = 1/2^+$ channel. We immediately find an outstanding feature in the $J^\pi = 1/2^+$ channel. Namely, our results by fss2 are very similar not to the AV18 results but to the AV18+UR($3N$) results shown in the parentheses. It is not surprising since fss2 gives the nearly correct binding energy without introducing the $3N$ force. On the other hand, the phase shift parameters of the $J^\pi = 3/2^+$ state are very similar between fss2 and AV18. In this state, the effect of the UR $3N$ force is very small owing to the Pauli principle. The difference between fss2 and AV18 is less than $0.2^\circ - 0.3^\circ$, which is comparable to the effect of the $3N$ force. For the P states, some of the eigenphase shifts show somewhat larger difference from the AV18 and AV18+UR($3N$) results especially at $E_n = 3$ MeV, but still less than 1° difference. After all, we have found good correspondence between our fss2 results and the predictions by the AV18+UR($3N$) potentials. The resemblance seen in Table I becomes more transparent if we calculate the J -averaged central phase shifts defined by Eq. (2·20) and compare them. The J -averaged central phase shifts can be used to evaluate the nd differential cross sections through Eqs. (2·21) and (2·22). We have illustrated these in Figs. 2 – 4 with dot-dashed curves, but they almost overlap with the solid curves for the exact calculations. We find that the D -wave components give an appreciable contribution to the differential cross sections even in such a low energy as $E_n=1$ MeV. This is of course because of the D -wave component of the deuteron wave function. This analysis encourages us to study the pd differential cross sections by a simple approximation for the Coulomb effect, discussed in § 2.2. We first assume that the nuclear scattering amplitude f_ℓ^N in Eq. (2·23) is equal to the nd scattering amplitude from the J -averaged central phase shift, $f_\ell = (e^{2i\delta_{\ell S_c}^C} - 1)/2iq_0$. This prescription yields fairly large overestimation of the differential cross sections as plotted in Figs. 2 – 4 with dotted curves. We find that a large effect of Coulomb modification on f_ℓ^N is necessary for the present low-energy pd scattering, which is a well-known fact claimed by many authors.^{34), 35), 44), 45)} Here, we use an extended version of the Coulomb externally corrected approximation,³⁵⁾ in which the nuclear eigenphase shifts for the pd scattering, $\delta_{\ell S_c}^C(pd)$, are calculated from our $\delta_{\ell S_c}^C(nd)$ by adding the difference of those evaluated with another NN interaction.

Table I. The nd eigenphase shifts and mixing parameters (in degrees), obtained from the model fss2. The maximum angular momentum for the NN system, $I_{\max} = 4$, and the momentum mesh points $n = 12-6-5$ are used. The corresponding parameters calculated by the Pisa group from the AV18 potential models are also listed for comparison.⁴²⁾ The parameters in the parentheses are predictions by the AV18+UR(3N) potentials.

| Model | fss2 | AV18 | fss2 | AV18 | fss2 | AV18 |
|----------------------|--------|----------|--------|----------|--------|----------|
| $E_n(\text{MeV})$ | 1.0 | 1.0 | 2.0 | 2.0 | 3.0 | 3.0 |
| ${}^4D_{1/2}$ | -0.978 | -0.980 | -2.52 | -2.53 | -3.82 | -3.85 |
| | — | (-0.976) | — | (-2.52) | — | (-3.84) |
| ${}^2S_{1/2}$ | -14.8 | -18.1 | -24.2 | -28.3 | -30.8 | -35.3 |
| | — | (-14.3) | — | (-24.0) | — | (-30.8) |
| $\eta_{1/2+}$ | 1.29 | 0.928 | 1.48 | 1.08 | 1.55 | 1.12 |
| | — | (1.39) | — | (1.47) | — | (1.45) |
| ${}^2P_{1/2}$ | -4.12 | -4.13 | -6.55 | -6.57 | -7.43 | -7.49 |
| | — | (-4.13) | — | (-6.58) | — | (-7.50) |
| ${}^4P_{1/2}$ | 11.8 | 12.0 | 19.3 | 19.9 | 23.6 | 24.2 |
| | — | (12.1) | — | (20.1) | — | (24.5) |
| $\varepsilon_{1/2-}$ | 3.50 | 3.47 | 5.02 | 4.98 | 6.76 | 6.68 |
| | — | (3.53) | — | (5.07) | — | (6.82) |
| ${}^4S_{3/2}$ | -46.6 | -46.7 | -60.5 | -60.8 | -69.6 | -69.9 |
| | — | (-46.6) | — | (-60.7) | — | (-69.7) |
| ${}^2D_{3/2}$ | 0.564 | 0.564 | 1.50 | 1.51 | 2.34 | 2.36 |
| | — | (0.564) | — | (1.51) | — | (2.36) |
| ${}^4D_{3/2}$ | -1.05 | -1.05 | -2.71 | -2.72 | -4.12 | -4.14 |
| | — | (-1.05) | — | (-2.71) | — | (-4.14) |
| $\varepsilon_{3/2+}$ | 0.603 | 0.621 | 0.688 | 0.686 | 0.763 | 0.747 |
| | — | (0.623) | — | (0.688) | — | (0.754) |
| $\xi_{3/2+}$ | 0.516 | 0.511 | 0.957 | 0.948 | 1.36 | 1.35 |
| | — | (0.514) | — | (0.948) | — | (1.35) |
| $\eta_{3/2+}$ | -0.106 | -0.107 | -0.232 | -0.231 | -0.363 | -0.363 |
| | — | (-0.105) | — | (-0.228) | — | (-0.356) |
| ${}^4F_{3/2}$ | 0.122 | 0.121 | 0.491 | 0.488 | 0.919 | 0.920 |
| | — | (0.121) | — | (0.489) | — | (0.921) |
| ${}^2P_{3/2}$ | -4.06 | -4.08 | -6.38 | -6.41 | -7.10 | -7.18 |
| | — | (-4.08) | — | (-6.43) | — | (-7.20) |
| ${}^4P_{3/2}$ | 13.7 | 13.9 | 21.9 | 22.3 | 25.5 | 26.0 |
| | — | (14.0) | — | (22.3) | — | (26.0) |
| $\varepsilon_{3/2-}$ | -1.28 | -1.24 | -1.93 | -1.86 | -2.72 | -2.62 |
| | — | (-1.27) | — | (-1.89) | — | (-2.66) |
| $\xi_{3/2-}$ | -0.196 | -0.177 | -0.334 | -0.262 | -0.427 | -0.265 |
| | — | (-0.177) | — | (-0.259) | — | (-0.256) |
| $\eta_{3/2-}$ | -1.04 | -1.00 | -2.17 | -2.17 | -3.57 | -3.52 |
| | — | (-1.04) | — | (-2.16) | — | (-3.53) |
| ${}^4G_{5/2}$ | -0.015 | -0.015 | -0.091 | -0.090 | -0.206 | -0.206 |
| ${}^2D_{5/2}$ | 0.560 | 0.559 | 1.49 | 1.49 | 2.31 | 2.33 |
| ${}^4D_{5/2}$ | -1.11 | -1.11 | -2.90 | -2.90 | -4.44 | -4.46 |
| $\varepsilon_{5/2+}$ | -0.263 | -0.277 | -0.291 | -0.297 | -0.312 | -0.315 |
| $\xi_{5/2+}$ | -0.233 | -0.272 | -0.491 | -0.494 | -0.716 | -0.701 |
| $\eta_{5/2+}$ | -0.659 | -0.821 | -1.42 | -1.49 | -2.02 | -2.04 |

Table I. — continued

| Model | fss2 | AV18 | fss2 | AV18 | fss2 | AV18 |
|----------------------|--------|--------|--------|--------|--------|--------|
| $E_n(\text{MeV})$ | 1.0 | 1.0 | 2.0 | 2.0 | 3.0 | 3.0 |
| $^4P_{5/2}$ | 13.1 | 13.2 | 21.4 | 21.7 | 25.8 | 26.0 |
| | — | (13.2) | — | (21.8) | — | (26.3) |
| $^2F_{5/2}$ | -0.063 | -0.063 | -0.251 | -0.251 | -0.465 | -0.466 |
| $^4F_{5/2}$ | 0.127 | 0.127 | 0.514 | 0.510 | 0.947 | 0.951 |
| $\varepsilon_{5/2-}$ | 0.399 | 0.447 | 0.479 | 0.472 | 0.514 | 0.538 |
| $\xi_{5/2-}$ | 0.384 | 0.390 | 0.690 | 0.684 | 0.938 | 0.926 |
| $\eta_{5/2-}$ | -0.117 | -0.123 | -0.239 | -0.239 | -0.343 | -0.334 |
| $^4D_{7/2}$ | -1.03 | -1.03 | -2.66 | -2.67 | -4.04 | -4.06 |
| $^2G_{7/2}$ | 0.0076 | 0.0075 | 0.047 | 0.047 | 0.108 | 0.107 |
| $^4G_{7/2}$ | -0.015 | -0.015 | -0.094 | -0.095 | -0.215 | -0.214 |
| $\varepsilon_{7/2+}$ | 0.230 | 0.325 | 0.353 | 0.368 | 0.355 | 0.355 |
| $\xi_{7/2+}$ | 0.362 | 0.427 | 0.781 | 0.798 | 1.16 | 1.14 |
| $\eta_{7/2+}$ | -0.106 | -0.143 | -0.287 | -0.299 | -0.459 | -0.459 |
| $^2F_{7/2}$ | -0.062 | -0.062 | -0.248 | -0.248 | -0.458 | -0.460 |
| $^4F_{7/2}$ | 0.132 | 0.132 | 0.533 | 0.532 | 1.00 | 1.00 |
| $\varepsilon_{7/2-}$ | -0.207 | 0.238 | -0.244 | -0.236 | -0.256 | -0.232 |
| $^2G_{9/2}$ | 0.075 | 0.0075 | 0.047 | 0.046 | 0.106 | 0.105 |
| $^4G_{9/2}$ | -0.015 | -0.016 | -0.097 | -0.097 | -0.223 | -0.223 |
| $\varepsilon_{9/2+}$ | -0.125 | -0.183 | -0.189 | -0.199 | -0.173 | -0.176 |
| $^4F_{9/2}$ | 0.124 | 0.124 | 0.497 | 0.496 | 0.921 | 0.922 |
| $^4G_{11/2}$ | -0.015 | -0.015 | -0.092 | -0.091 | -0.208 | -0.208 |

Table II. The nd J -averaged central phase shifts (in degrees), calculated from the eigenphase shifts in Table I through Eq. (2·20). The others are the same as Table I.

| Model | fss2 | AV18 | fss2 | AV18 | fss2 | AV18 |
|-------------------|---------|---------|--------|---------|--------|---------|
| $E_n(\text{MeV})$ | 1.0 | 1.0 | 2.0 | 2.0 | 3.0 | 3.0 |
| 2S | -14.8 | -18.1 | -24.2 | -28.3 | -30.8 | -35.3 |
| | — | (-14.3) | — | (-24.0) | — | (-30.8) |
| 2P | -4.08 | -4.10 | -6.44 | -6.46 | -7.21 | -7.28 |
| | — | (-4.10) | — | (-6.48) | — | (-7.30) |
| 2D | 0.562 | 0.562 | 1.49 | 1.50 | 2.32 | 2.34 |
| 2F | -0.0626 | -0.0624 | -0.249 | -0.249 | -0.462 | -0.463 |
| 4S | -46.6 | -46.7 | -60.5 | -60.8 | -69.6 | -69.9 |
| | — | (-46.6) | — | (-60.7) | — | (-69.7) |
| 4P | 13.1 | 13.2 | 21.2 | 21.6 | 25.3 | 25.7 |
| | — | (13.3) | — | (21.7) | — | (25.9) |
| 4D | -1.05 | -1.05 | -2.73 | -2.74 | -4.15 | -4.18 |
| 4F | 0.127 | 0.127 | 0.510 | 0.508 | 0.948 | 0.950 |

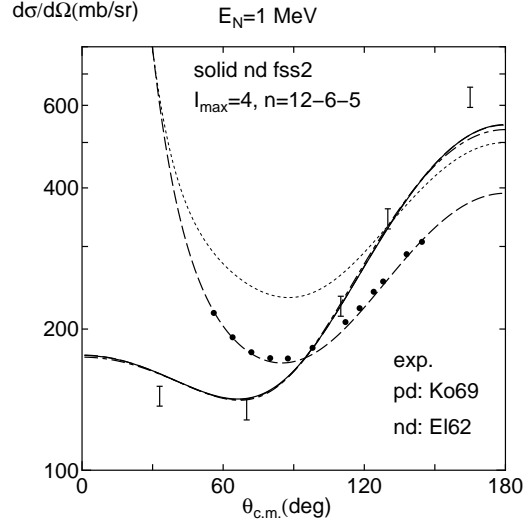


Fig. 2. fss2 predictions to the nd and pd differential cross sections obtained from various prescriptions for the phase shifts at $E_N=1$ MeV: the exact nd calculation (solid curve), the J -averaged central phase shifts (dot-dashed curve), the Coulomb externally corrected approximation with $\delta^N = \delta(nd)$ (dotted curve), and the Coulomb modified nuclear phase shifts in Table III (dashed curve). The experimental data are taken from Ref. 48) for El62 (nd with errorbars) and Ref. 49) for Ko69 (pd with filled circles).

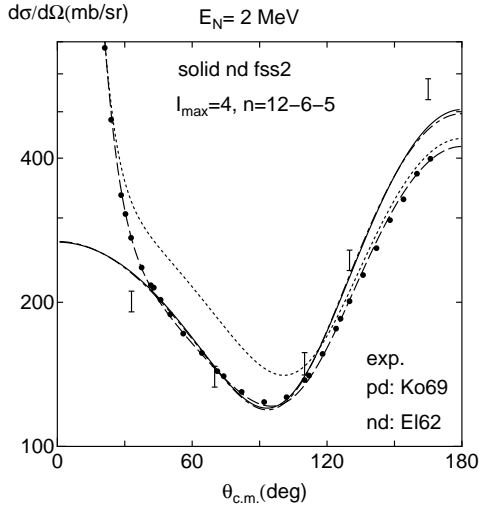


Fig. 3. The same as Fig. 2, but for $E_N=2$ MeV.

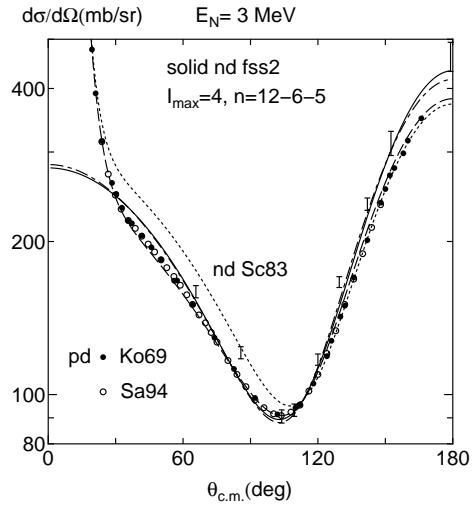


Fig. 4. The same as Fig. 2., but for $E_N=3$ MeV. The experimental data are taken from Ref. 50) for Sc83 (nd with errorbars) and Ref. 51) for Sa94 (pd with empty circles).

Table III. The Coulomb modified J -averaged central phase shifts (in degrees), $\delta^N = \delta_{\ell S_c}^C(nd) + \Delta_\ell$, used for the calculations of the pd differential cross sections in Figs. 2 – 4. Here, $\delta_{\ell S_c}^C(nd)$ are given in Table II and $\Delta_\ell = [\delta_{\ell S_c}^C(pd) - \delta_{\ell S_c}^C(nd)]_{\text{AV18}}$ are evaluated from Ref. 42). The results of the phase shift analysis (PSA) at $E_N = 3$ MeV are also shown for comparison.

| $E_N(\text{MeV})$ | 1.0 | | 2.0 | | 3.0 | | 3.0 (PSA) | 3.0 (PSA) |
|-------------------|---------------|------------|---------------|------------|---------------|------------|-------------------|-------------------|
| | Δ_ℓ | δ^N | Δ_ℓ | δ^N | Δ_ℓ | δ^N | Ref. 42) | Ref. 41) |
| 2S | 4.9 | -9.9 | 4.1 | -20.1 | 3.1 | -27.7 | -24.85 ± 0.23 | -24.87 ± 0.28 |
| 4S | 9.7 | -36.9 | 7.8 | -52.7 | 6.8 | -62.8 | -63.80 ± 0.11 | -63.95 ± 0.28 |
| 4P | -3.1 | 10.0 | -2.6 | 18.6 | -2.0 | 23.3 | 23.86 ± 0.01 | 23.37 ± 0.11 |

The Coulomb correction can be evaluated since the nd and pd eigenphase shifts for $E_N = 1, 2$ and 3 MeV by the AV18 potential (or the AV18+UR(3N) potentials) are both given in Tables 1 and 2 of Ref. 42), respectively. The J -averaged central phase shifts calculated from these values imply that the Coulomb modification is significant (more than 1°) only for the 2S , 4S and 4P channels. The difference $\Delta_\ell = [\delta_{\ell S_c}^C(pd) - \delta_{\ell S_c}^C(nd)]_{\text{AV18}}$ listed in Table III is obtained in this way. The pd differential cross sections calculated with these Coulomb modified nuclear scattering amplitude f_ℓ^N are plotted in Figs. 2 – 4 with dashed curves. We find excellent agreement with the experimental data for the pd differential cross sections with the aid of the AV18 Coulomb effect. The overestimation in the case of the original Coulomb externally corrected approximation is improved mainly by $7^\circ - 10^\circ$ modification of the 4S phase shift to the attractive direction (see Table III). These analyses imply that the correct treatment of the Coulomb force could reproduce the pd experimental data for the differential cross sections without reinforcing fss2 with the $3N$ force.

3.2. The nd effective range parameters

Since the good correspondence between fss2 and AV18+UR(3N) are found in the eigenphase shifts, we can expect that the S -wave effective range parameters for the spin-doublet and quartet channels should also be reproduced by fss2 without introducing the $3N$ force. These are determined from Eq. (2.24) for the quartet channel and Eq. (2.25) for the doublet channel. The S -wave effective range parameters are obtained by using Schlessinger's point method⁵²⁾ (a type of Pade approximation) to the effective-range function $K(q_0) = q_0 \cot\delta$. This method is convenient to approximate a function with a pole such as the doublet effective-range function and to take into account the contributions of the higher order terms in Eqs. (2.24) and (2.25) in a natural way. It is very hard in the momentum representation to maintain sufficient accuracy of the eigenphase shift for the extremely low energies if we use the realistic deuteron wave function including the D -wave component. We therefore use the sample points of energies between $E_{\text{cm}} = 200$ keV and 2 MeV shown in Figs. 5 (the doublet channel) and 6 (the quartet channel) unless the denominator in the Schlessinger's point method hits zeros. In order to obtain the eigenphase shifts with accuracy of less than 0.01° , we need to take fine mesh points of p for the NN relative motion. We use a set of mesh points $n=6-10-5$ and the NN partial waves up to G -wave ($I_{\text{max}} = 4$). A typical example of fitting to $K(q_0)$ is shown in Figs. 5 and 6. We reconfirm a pole structure existing in the doublet channel at

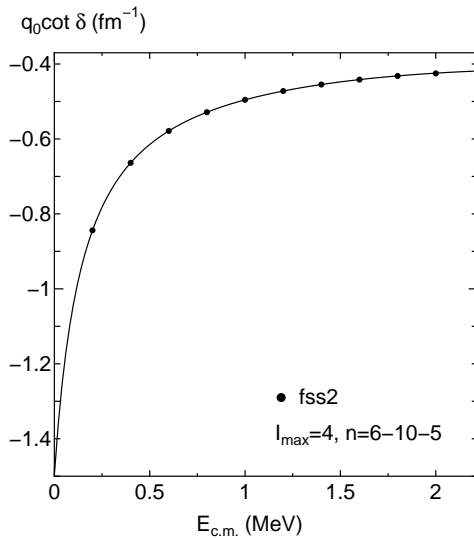


Fig. 5. The effective-range function $K(q_0) = q_0 \cot \delta$ for the doublet S -state as a function of E_{cm} . The curve shows the rational approximation made by the Schlessinger's point method.⁵²⁾

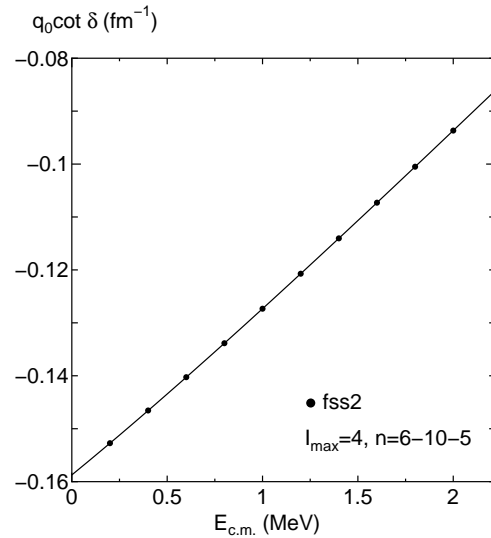


Fig. 6. The same as Fig. 5, but $K(q_0) = q_0 \cot \delta$ for the quartet S -state.

$$E_Q = -(3\hbar^2 q_Q^2 / 4M) \simeq -150 \text{ keV.}$$

Table IV lists the model-space dependence of the triton binding energy and effective range parameters. As to the almost converged triton binding energy $E_B(^3\text{H}) = 8.311 \text{ MeV}$ with $I_{\text{max}} = 6$, the small difference from the original result of fss2 (8.326 MeV with $I_{\text{max}} = 6$)¹¹⁾ comes mainly from the nonlocal Gaussian approximation to the interaction kernel, adopted in this study. Since we have three NN pairs in the triton, this 15 keV difference in the triton binding energy is consistent with the 4 keV difference in the deuteron binding energy, which is the difference of 2.2250 MeV (the original result of fss2)⁶⁾ and 2.2206 MeV (the result of the nonlocal Gaussian potential based on fss2). We find that the spin-quartet scattering length $^4a_{nd}$ is quite insensitive to the model space adopted. This insensitivity is related to the small distortion effect of the deuteron due to the Pauli repulsion of the nd interaction in this channel, which is a kinematical constraint from the spin-isospin quantum numbers. The system is therefore independent of the details of the NN interaction. On the other hand, the spin-doublet scattering length $^2a_{nd}$ is subject to a strong channel coupling effect as seen in Table IV. We find that the simplest five-channel ($S + D$) calculation, incorporating the $^3S_1 + ^3D_1$ and 1S_0 NN channels only, yields a value very close to the converged one. However, this is quite accidental and the well converged value is achieved after many partial waves, up to the G -wave of NN interaction at least, are included. The values of $|E_Q| / (^2a_{nd}) \sim 220 \text{ keV/fm}$ are al-

Table IV. The triton binding energy $E_B(^3\text{H})$ and S -wave effective range parameters, $^2a_{nd}$, $(^2r_e)_{nd}$, $^4a_{nd}$ and $(^4r_e)_{nd}$, predicted by fss2 for various model spaces with the maximum angular momentum of the NN interaction (I_{\max}) included. The nonlocal Gaussian potential with 15-point quadrature is used for fss2. In “ $S + D$ ”, the $^3S_1 + ^3D_1$ and 1S_0 NN channels are only included. The pole energy for the doublet channel, E_Q , is also shown. The calculated deuteron binding energy is 2.2206 MeV. The momentum mesh points with $n=6-10-5$ are used.

| I_{\max} | $E_B(^3\text{H})$ (MeV) | $^2a_{nd}$ (fm) | $(^2r_e)_{nd}$ (fm) | E_Q (keV) | $^4a_{nd}$ (fm) | $(^4r_e)_{nd}$ (fm) |
|------------|-------------------------|-----------------|---------------------|-------------|-----------------|---------------------|
| $S + D$ | 8.247 | 0.65 | -149 | -147 | 6.30 | 1.84 |
| 1 | 7.948 | 0.94 | -102 | -207 | 6.31 | 1.85 |
| 2 | 8.213 | 0.72 | -133 | -163 | 6.30 | 1.84 |
| 3 | 8.298 | 0.67 | -146 | -151 | 6.30 | 1.84 |
| 4 | 8.307 | 0.66 | -148 | -148 | 6.30 | 1.84 |

Table V. Comparison of the nd scattering lengths, predicted by using fss2 ($I_{\max} = 4$), with other models. For the fss2 results, the charge dependence of the NN force is neglected. The heading NN implies the calculation using only the NN force, and NN +TM99 the calculation including the Tucson-Melbourne 99 (TM99) 2π -exchange $3N$ force.^{53),54)} The results by CD-Bonn 2000, AV18 and Nijm I for the NN force are taken from Ref. 23) ($I_{\max} = 5$). The experimental values are taken from Ref. 25). The values of $^4a_{nd}$ are insensitive to the $3N$ force.

| model | $E_B(^3\text{H})$ (MeV) | | $^2a_{nd}$ (fm) | | $^4a_{nd}$ (fm) |
|--------------|-------------------------|------------|-----------------|------------|-----------------|
| | NN | NN +TM99 | NN | NN +TM99 | NN (+TM99) |
| fss2 | 8.307 | — | 0.66 | — | 6.30 |
| CD-Bonn 2000 | 8.005 | 8.482 | 0.925 | 0.569 | 6.347 |
| AV18 | 7.628 | 8.482 | 1.248 | 0.587 | 6.346 |
| Nijm I | 7.742 | 8.485 | 1.158 | 0.594 | 6.342 |
| exp | 8.482 | | 0.65 ± 0.04 | | 6.35 ± 0.02 |

most independent of the model space. This linear correlation is already suggested in Ref. 32) for the separable potentials. A strong correlation between $E_B(^3\text{H})$ and $^2a_{nd}$ is also apparent in Table IV.

In Table V, we compare $E_B(^3\text{H})$ and $^2a_{nd}$ by fss2 with other calculations using meson-exchange potentials including the $3N$ force.²³⁾ Here, fss2 does not incorporate the charge dependence of the NN interaction, but the other calculations in Table V include this effect. As in $E_B(^3\text{H})$, it should give an appreciable influence to $^2a_{nd}$. We will estimate the maximum shift of $^2a_{nd}$ by simply assuming the same correlation as Phillips line for the triton binding energy. For fss2, the slope of the Phillips line, -0.686 fm/MeV, yields 0.13 fm for the charge dependence effect of the triton binding energy 190 keV.⁵⁵⁾ After the charge dependence correction, $^2a_{nd}$ for fss2 would turn out to be $^2a_{nd} \sim 0.76 - 0.80$ fm. Table V shows that the effect of the $3N$ force is more important than the charge dependence of the NN force. When NN meson-exchange potentials are only used, $^2a_{nd}$ is more than 0.9 fm. The experimental values for $^2a_{nd}$ and $E_B(^3\text{H})$ are reproduced only when the $3N$ force is included. The model fss2 almost reproduces $E_B(^3\text{H})$ and $^2a_{nd}$ simultaneously without introducing the $3N$ force. We should keep in mind that the mechanism to reproduce $^2a_{nd}$ is

Table VI. The quartet ($S_c = 3/2$) and doublet ($S_c = 1/2$) S -wave contributions to the total cross sections σ_{tot} , calculated from the effective range parameters for fss2 with $I_{\text{max}} = 4$ in Table IV. The calculated total cross sections σ_{tot} are taken from Ref. 14).

| E_n | 0 MeV | 1 MeV | 2 MeV | 3 MeV |
|----------------------------|------------------------------------|--|---|--|
| 4S (mb) | 3325 (99.5%) | 2055 (72%) | 1467 (59%) | 1128 (54%) |
| 2S (mb) | 18.2 (0.54%) | 122.4 (4.3%) | 158.4 (6.3%) | 165.5 (7.9%) |
| S -wave (mb) | 3343 | 2177 (77%) | 1625 (66%) | 1294 (62%) |
| σ_{tot} (mb) | 3185 (0.15 MeV) | 2833 | 2480 | 2104 |
| exp. (mb) | $3120 \pm 180^{56)}$ (0.07 MeV) | $2893.6 \pm 18.2^{57)}$ $2854 \pm 39^{58)}$ $3110 \pm 200^{59)}$ | $2550.6 \pm 11.1^{57)}$ $2537 \pm 10^{56)}$ $2600 \pm 80^{59)}$ | $2158.0 \pm 7.2^{57)}$ $2240 \pm 90^{59)}$ $2160 \pm 86^{60)}$ |

quite different from that in the spin-quartet case. The large positive value for ${}^4a_{nd}$ is related to the Pauli repulsion for the loosely-bound deuteron cluster. On the other hand, the value of ${}^2a_{nd}$ is entirely from the dynamical origin related to the fairly large triton binding energy $E_B^{\text{exp}}({}^3\text{H}) = 8.482$ MeV and the existence of the pole structure in the effective-range function just below the elastic threshold. In this special situation, it is natural that more attractive nd interaction, afforded by the $3N$ force in the meson-exchange potentials or by fss2 without the $3N$ force, can reproduce a smaller value for ${}^2a_{nd}$, which is the content of the Phillips line.

In Table VI, we show the S -wave contributions from the quartet ($S_c = 3/2$) and doublet ($S_c = 1/2$) channels to the total cross sections, calculated from the effective range parameters for fss2 with $I_{\text{max}} = 4$ in Table IV. We find that the total cross sections are dominated by the S -wave contribution, which is more than 60% even for $E_n = 3$ MeV. Furthermore, the quartet state is far more important than the doublet state due to the small values of $|q_0 \cot \delta|$, even considering the statistical weight factor $(2S_c + 1)$. As the energy increases, the contribution from the doublet state becomes appreciable owing to avoiding the pole structure just below the elastic threshold, but is still less than 10% at $E_n=3$ MeV. This implies a very special situation that an extra attraction to the ${}^2S_{1/2}$ state by the $3N$ force is unimportant to reproduce the differential cross sections of the low-energy nd scattering, and they are mainly determined by the magnitude of the repulsive ${}^4S_{3/2}$ eigenphase shift.

§4. Summary

Motivated by the success of the QM baryon-baryon interaction fss2 reproducing the triton binding energy almost correctly without the $3N$ force,¹¹⁾ we have extended the Faddeev calculation to the low-energy nd scattering by employing a new algorithm¹⁴⁾ to solve the Alt-Grassberger-Sandahs equation.³³⁾ The QM NN interaction, formulated in the two-cluster RGM, has rich contents of nonlocality that the standard meson-exchange potentials do not possess.⁶⁾ In addition to the dominant nonlocality from the RGM interaction kernel, an extra nonlocality emerges from the off-shell transformation to eliminate the energy dependence connected to the normalization kernel,¹²⁾ which is sometimes neglected in similar works.^{24), 28)} To reduce

the computation time for three-body calculations, we have developed and used the nonlocal Gaussian potential constructed from the model fss2.¹³⁾ The nonlocality and the energy dependence of fss2 is, however, strictly preserved in this potential model, resulting in an almost the same amount of the triton binding energy with only 15 keV less.

In this paper, we have examined the effective range parameters of the nd scattering and the low-energy differential cross sections below the deuteron breakup threshold. The elastic scattering amplitudes in the channel-spin representation are parameterized by the eigenphase shifts and mixing parameters,¹⁵⁾ from which the S -wave effective range parameters are derived by employing the single-channel effective range formula. We have reconfirmed that the improved single-channel effective range formula should be used for the channel-spin doublet ($S_c = 1/2$) state, to incorporate the pole structure of the effective-range function, existing just below the elastic threshold.²⁹⁾⁻³²⁾ The predicted effective range parameters by fss2 are: ${}^2a_{nd} = 0.66$ fm, $({}^2r_e)_{nd} \sim -150$ fm, $E_Q = -(3\hbar^2 q_Q^2/4M) \sim -150$ keV, and ${}^4a_{nd} = 6.30$ fm, $({}^4r_e)_{nd} = 1.84$ fm without the charge dependence of the NN interaction. After the charge dependence correction, ${}^2a_{nd}$ for fss2 would turn out to be ${}^2a_{nd} \sim 0.76 - 0.80$ fm. It is found that the almost same ${}^2a_{nd}$ value is accidentally obtained in the restricted model space involving only the ${}^3S_1 + {}^3D_1$ and 1S_0 NN interaction. However, the deuteron distortion effect in the spin doublet channel is so strong that the sufficient partial waves, up to the G -wave at least, are necessary to obtain the converged result. On the other hand, the positive value ${}^4a_{nd} \sim 6.3$ fm, implying the repulsive nature of the nd interaction in the spin quartet ($S_c = 3/2$) channel, is quite insensitive to the expansion of the model space, owing to the kinematical constraint by the effect of the Pauli principle.

A detailed comparison of the nd eigenphase shifts predicted by fss2 and by the AV18 plus the UR $3N$ potential⁴²⁾ shows a prominent resemblance especially for the ${}^2S_{1/2}$ state. The UR $3N$ potential gives a sizable effect only on the $J^\pi = 1/2^+$ channel, while very small effects on the ${}^4S_{3/2}$ state and the other partial waves. We find reasonable agreement with the nd experimental data for the low-energy differential cross sections. Since the pd data are more precise than the nd data, we have also examined the differential cross sections of the pd elastic scattering. We have employed a simple prescription adding the Coulomb amplitude to the nd scattering amplitudes with the factor $e^{i(\sigma_\ell + \sigma_{\ell'})}$, which is called the Coulomb externally corrected approximation.^{34),35)} The assumption using the nd scattering amplitude with no modification gives too large differential cross sections for $E_p = 1 - 3$ MeV, which implies that the Coulomb modification of the nuclear phase shifts is very important in this low-energy region. The Coulomb modified nuclear phase shifts are evaluated by adding the major difference of the nd and pd eigenphase shifts predicted by the AV18 potential.⁴²⁾ The modification is carried out with respect to the J -averaged central phase shifts only for the 2S , 4S and 4P channels. We have found agreement with the experimental data for the pd differential cross sections at $E_p = 1, 2$ and 3 MeV. Since the ${}^4S_{3/2}$ contribution is dominant in the differential cross sections below the deuteron breakup threshold, the ${}^4S_{3/2}$ eigenphase shift of the nd (and probably

pd) elastic scattering is properly predicted by fss2.

Based on these analyses, we can conclude that the spin-doublet low-energy eigenphase shift predicted by fss2 is sufficiently attractive to reproduce predictions of the AV18 plus Urbana $3N$ force, yielding the observed value of the doublet scattering length and the correct nd and pd differential cross sections below the deuteron breakup threshold. These results are in accordance with the bound-state calculation of the triton, in which fss2 predicts a nearly correct binding energy close to the experimental value without introducing the $3N$ force.¹¹⁾ It is important to examine if the correct treatment of the Coulomb force for fss2 can reproduce the pd differential cross sections and the polarization observables below the deuteron breakup threshold.

Acknowledgments

The authors would like to thank Professor B. F. Gibson and Professor S. Ishikawa for informing them on the pole structure of the spin-doublet effective-range function. They also thank Professor K. Sagara for providing them the pd experimental data taken by the Kyushu University group. This work was supported by the Grant-in-Aid for Scientific Research on Priority Areas (Grant No. 2002803), and by the Grant-in-Aid for the Global COE Program “The Next Generation of Physics, Spun from Universality and Emergence” from the Ministry of Education, Culture, Sports, Science and Technology (MEXT) of Japan. It was also supported by the core-stage backup subsidies of Kyoto University. The numerical calculations were carried out on Altix3700 BX2 at YITP in Kyoto University.

Appendix A

— The spin-isospin factors and the rearrangement coefficients in Eq. (2·6) —

In this appendix, we give the rearrangement coefficients $g_{\gamma,\gamma'}(q, q', x)$ in Eq. (2·6) for the permutation operator $P = P_{(123)} + P_{(123)}^2$, together with the spin-isospin factors for the $3N$ system. The two contributions from $P_{(123)} = P_{(12)}P_{(23)}$ and $P_{(123)}^2 = P_{(13)}P_{(23)}$ become equal owing to the Pauli principle for the particle 1 and particle 2. We therefore only need to calculate the rearrangement coefficients for $(-2)P_{(13)}$. These are given by

$$g_{\gamma,\gamma'}(q, q', x) = \sum_{\lambda_1+\lambda_2=\lambda} \sum_{\lambda'_1+\lambda'_2=\lambda'} q^{\lambda'_1+\lambda_2} q'^{\lambda_1+\lambda'_2} \left(\frac{1}{2}\right)^{\lambda_2+\lambda'_2} \sum_k (2k+1) g_{\gamma,\gamma'}^{\lambda_1\lambda'_1 k} P_k(x), \quad (\text{A}\cdot 1)$$

with

$$g_{\gamma,\gamma'}^{\lambda_1\lambda'_1 k} = \sum_{LS} (X_N)_{\gamma,\gamma'}^{LSJ} G_{(\lambda\ell),(\lambda'\ell')}^{\lambda_1\lambda'_1 kL}, \quad (\text{A}\cdot 2)$$

and $P_k(x)$ being Legendre polynomials. The spatial rearrangement factor $G_{(\lambda\ell),(\lambda'\ell')}^{\lambda_1\lambda'_1kL}$ is given by

$$\begin{aligned} G_{(\lambda\ell),(\lambda'\ell')}^{\lambda_1\lambda'_1kL} &= G_{(\lambda'\ell'),(\lambda\ell)}^{\lambda'_1\lambda_1kL} = 4\pi \left[\frac{(2\lambda+1)!(2\lambda'+1)!}{(2\lambda_1+1)!(2\lambda_2+1)!(2\lambda'_1+1)!(2\lambda'_2+1)!} \right]^{\frac{1}{2}} \\ &\times \int d\hat{\mathbf{q}}d\hat{\mathbf{q}}' [Y_{(\lambda_1\lambda_2)\lambda}(\hat{\mathbf{q}}', \hat{\mathbf{q}})Y_\ell(\hat{\mathbf{q}})]_{LM}^* P_k(\hat{\mathbf{q}} \cdot \hat{\mathbf{q}}') [Y_{(\lambda'_1\lambda'_2)\lambda'}(\hat{\mathbf{q}}, \hat{\mathbf{q}}')Y_{\ell'}(\hat{\mathbf{q}}')]_{LM} \\ &= \left[\frac{(2\lambda+1)!(2\lambda'+1)!}{(2\lambda_1)!(2\lambda_2)!(2\lambda'_1)!(2\lambda'_2)!} \right]^{\frac{1}{2}} \widehat{\lambda}\widehat{\lambda}'\widehat{\ell}' \sum_{ff'} \langle \lambda_2 0 \ell 0 | f 0 \rangle \langle \lambda'_2 0 \ell' 0 | f' 0 \rangle \langle k 0 \lambda_1 0 | f' 0 \rangle \\ &\times \langle k 0 \lambda'_1 0 | f 0 \rangle \begin{Bmatrix} f & L & \lambda_1 \\ \lambda & \lambda_2 & \ell \end{Bmatrix} \begin{Bmatrix} f' & L & \lambda'_1 \\ \lambda' & \lambda'_2 & \ell' \end{Bmatrix} \begin{Bmatrix} \lambda'_1 & f' & L \\ \lambda_1 & f & k \end{Bmatrix}. \end{aligned} \quad (\text{A}\cdot 3)$$

Here, $\widehat{\lambda} = \sqrt{2\lambda+1}$ etc. and $\lambda_2 = \lambda - \lambda_1$, $\lambda'_2 = \lambda' - \lambda'_1$ with $\lambda_1 = 0 - \lambda$, $\lambda'_1 = 0 - \lambda'$. The explicit expression of the spin-isospin factors $(X_N)_{\gamma,\gamma'}^{LSJ}$ depends on the channel specification scheme. For the LS coupling scheme

$$\langle \widehat{\mathbf{p}}, \widehat{\mathbf{q}}; 123 | \gamma \rangle = \left[Y_{(\lambda\ell)L}(\widehat{\mathbf{p}}, \widehat{\mathbf{q}}) \left[\chi_{st}(1, 2) \chi_{\frac{1}{2}\frac{1}{2}}(3) \right]_{SS_z; \frac{1}{2}T_z} \right]_{JJ_z}, \quad (\text{A}\cdot 4)$$

with $\gamma = [(\lambda\ell)L(s\frac{1}{2})S]JJ_z; (t\frac{1}{2})\frac{1}{2}T_z$, we do not need the LS sum in Eq. (A·2), since the orbital angular momentum L and the total spin S are both conserved. We modify Eq. (A·2) to

$$(X_N)_{\gamma,\gamma'}^{LSJ} \rightarrow \left(X_N^{S\frac{1}{2}} \right)_{st,s't'}^{LSJ} \equiv -2X_{s,s'}^S X_{t,t'}^{\frac{1}{2}}, \quad (\text{A}\cdot 5)$$

where a common definition of the spin and isospin factors

$$X_{s,s'}^{\frac{3}{2}} = \begin{pmatrix} 0 & 0 \\ 0 & 1 \end{pmatrix}, \quad X_{s,s'}^{\frac{1}{2}} = \begin{pmatrix} \frac{1}{2} & -\frac{\sqrt{3}}{2} \\ -\frac{\sqrt{3}}{2} & -\frac{1}{2} \end{pmatrix}, \quad (\text{A}\cdot 6)$$

is used. In Eq. (A·6), the upper row (or the left-most column) corresponds to $s=0$ ($s'=0$) and the second row (or the right-most column) corresponds to $s=1$ ($s'=1$). For the jj -coupling scheme

$$\langle \widehat{\mathbf{p}}, \widehat{\mathbf{q}}; 123 | \gamma \rangle = \left[[Y_\lambda(\widehat{\mathbf{p}})\chi_{st}(1, 2)]_I [Y_\ell(\widehat{\mathbf{q}})\chi_{\frac{1}{2},\frac{1}{2}}(3)]_j \right]_{JJ_z; \frac{1}{2}T_z}, \quad (\text{A}\cdot 7)$$

with $\gamma = [(\lambda s)I(\ell\frac{1}{2})j]JJ_z; (t\frac{1}{2})\frac{1}{2}T_z$, we use the superposition of Eq. (A·2) with

$$(X_N)_{\gamma,\gamma'}^{LSJ} = \begin{bmatrix} \lambda & s & I \\ \ell & \frac{1}{2} & j \\ L & S & J \end{bmatrix} \begin{bmatrix} \lambda' & s' & I' \\ \ell' & \frac{1}{2} & j' \\ L & S & J \end{bmatrix} \left(X_N^{S\frac{1}{2}} \right)_{st,s't'}^{LSJ}. \quad (\text{A}\cdot 8)$$

The coefficients in the channel-spin formalism with Eq. (2·3) are similarly obtained as

$$(X_N)_{\gamma,\gamma'}^{LSJ} = \sum_{jj'} \begin{bmatrix} 0 & \ell & \ell \\ I & \frac{1}{2} & S_c \\ I & j & J \end{bmatrix} \begin{bmatrix} \lambda & s & I \\ \ell & \frac{1}{2} & j \\ L & S & J \end{bmatrix} \begin{bmatrix} 0 & \ell' & \ell' \\ I' & \frac{1}{2} & S'_c \\ I' & j' & J \end{bmatrix} \begin{bmatrix} \lambda' & s' & I' \\ \ell' & \frac{1}{2} & j' \\ L & S & J \end{bmatrix}$$

$$\times \left(X_N^{S\frac{1}{2}} \right)_{st,s't'}^{LSJ}. \quad (\text{A}\cdot 9)$$

For the practical calculations, it is convenient first to calculate the product of one 6- j and one 9- j coefficients defined through

$$A_{(\ell S_c)(\lambda_s)I}^{LSJ} = \sum_j (-1)^{I+\ell+S_c+j} \widehat{S}_c \widehat{j} \begin{Bmatrix} \frac{1}{2} & S_c & I \\ J & j & \ell \end{Bmatrix} \begin{bmatrix} \lambda & s & I \\ \ell & \frac{1}{2} & j \\ L & S & J \end{bmatrix}. \quad (\text{A}\cdot 10)$$

Furthermore, the factor 2 will be taken off to cancel with the 1/2 factor over the x integral. Then we use for Eq. (A.2)

$$\frac{1}{2} g_{\gamma,\gamma'}^{\lambda_1\lambda'_1 k} = -X_{t,t'}^{\frac{1}{2}} \sum_{LS} A_{(\ell S_c)(\lambda_s)I}^{LSJ} A_{(\ell' S'_c)(\lambda'_s)I'}^{LSJ} X_{s,s'}^S G_{(\lambda\ell),(\lambda'\ell')}^{\lambda_1\lambda'_1 k L}. \quad (\text{A}\cdot 11)$$

References

- 1) D. Hüber, W. Glöckle, J. Golak, H. Witała, H. Kamada, A. Kievsky, S. Rosati and M. Viviani, Phys. Rev. C **51** (1995), 1100.
- 2) See for example, H. Kamada, A. Nogga, W. Glöckle, E. Hiyama, M. Kamimura, K. Varga, Y. Suzuki, M. Viviani, A. Kievsky, S. Rosati, J. Carlson, S. C. Pieper, R. B. Wiringa, P. Navrátil, B. R. Barrett, N. Barnea, W. Leidemann and G. Orlandini, Phys. Rev. C **64** (2001), 044001, and references therein.
- 3) A. Nogga, H. Kamada and W. Glöckle, Phys. Rev. Lett. **85** (2000), 944.
- 4) E. Epelbaum, H. Kamada, A. Nogga, H. Witała, W. Glöckle and Ulf-G. Meißner, Phys. Rev. Lett. **86** (2001), 4787.
- 5) E. Epelbaum, A. Nogga, W. Glöckle, H. Kamada, Ulf-G. Meißner and H. Witała, Phys. Rev. C **66** (2002), 064001.
- 6) Y. Fujiwara, Y. Suzuki and C. Nakamoto, Prog. Part. Nucl. Phys. **58** (2007), 439.
- 7) Y. Fujiwara, T. Fujita, M. Kohno, C. Nakamoto and Y. Suzuki, Phys. Rev. C **65** (2002), 014002.
- 8) Y. Fujiwara, Y. Suzuki, M. Kohno and K. Miyagawa, Phys. Rev. C **66** (2002), 021001(R).
- 9) Y. Fujiwara, K. Miyagawa, Y. Suzuki, M. Kohno and H. Nemura, Nucl. Phys. A **721** (2003), 983c.
- 10) Y. Fujiwara, Y. Suzuki, M. Kohno and K. Miyagawa, Phys. Rev. C **70** (2004), 024001.
- 11) Y. Fujiwara, Y. Suzuki, M. Kohno and K. Miyagawa, Phys. Rev. C **77** (2008), 027001.
- 12) Y. Suzuki, H. Matsumura, M. Orabi, Y. Fujiwara, P. Descouvemont, M. Theeten and D. Baye, Phys. Lett. B **659** (2008), 160.
- 13) K. Fukukawa, Y. Fujiwara and Y. Suzuki, Mod. Phys. Lett. A **24** (2009), 1035.
- 14) Y. Fujiwara and K. Fukukawa, Prog. Theor. Phys. **124** (2010), 433.
- 15) R. G. Seyler, Nucl. Phys. A **124** (1969), 253.
- 16) A. C. Phillips, Rep. Prog. Phys. **40** (1977), 905; Nucl. Phys. A **107** (1968), 209.
- 17) J. L. Friar, B. F. Gibson, G. L. Payne and C. R. Chen, Phys. Rev. C **30** (1984), 1121.
- 18) C. R. Chen, G. L. Payne, J. L. Friar and B. F. Gibson, Phys. Rev. C **33** (1986), 401.
- 19) C. R. Chen, G. L. Payne, J. L. Friar and B. F. Gibson, Phys. Rev. C **39** (1989), 1261.
- 20) C. R. Chen, G. L. Payne, J. L. Friar and B. F. Gibson, Phys. Rev. C **44** (1991), 50.
- 21) A. Kievsky, M. Viviani and S. Rosati, Nucl. Phys. A **577** (1994), 511.
- 22) A. Kievsky, Nucl. Phys. A **624** (1997), 125.
- 23) H. Witała, A. Nogga, H. Kamada, W. Glöckle, J. Golak and R. Skibiński, Phys. Rev. C **68** (2003), 034002.
- 24) H. Garcialazo and A. Valcarce, Phys. Rev. C **76** (2007), 057002.
- 25) W. Dilg, L. Koester and W. Nistler, Phys. Lett. B **36** (1971), 208.
- 26) D. R. Entem, F. Fernández and A. Valcarce, Phys. Rev. C **62** (2000), 034002.
- 27) A. Valcarce, H. Garcilazo, F. Fernández and P. Gonzáles, Rep. Prog. Phys. **68** (2005), 965.

- 28) B. Juliá-Díaz, J. Haidenbauer, A. Valcarce and F. Fernández, Phys. Rev. C **65** (2002), 034001.
- 29) L. M. Delves, Phys. Rev. **118** (1960), 1318.
- 30) G. Barton and A. C. Phillips, Nucl. Phys. A **132** (1969), 97.
- 31) A. S. Reiner, Phys. Lett. B **28** (1969), 387.
- 32) J. S. Whiting and M. G. Fuda, Phys. Rev. C **14** (1976), 18.
- 33) E. O. Alt, P. Grassberger and W. Sandhas, Nucl. Phys. B **2** (1967), 167.
- 34) P. Doleschall, W. Grüebler, V. König, P. A. Schmelzbach, F. Sperisen and B. Jenny, Nucl. Phys. A **380** (1982), 72.
- 35) A. Deltuva, A. C. Fonseca and P. U. Sauer, Phys. Rev. C **71** (2005), 054005.
- 36) W. Glöckle, *The Quantum Mechanical Few-Body Problem, Texts and Monographs in Physics* (Springer, Berlin, 1983).
- 37) W. Glöckle, H. Witała, D. Hüber, H. Kamada and J. Golak, Phys. Rep. **274** (1996), 107.
- 38) P. A. Schmelzbach, W. Glüebler, R. E. White, V. König, R. Risler and P. Marmier, Nucl. Phys. A **197** (1972), 273.
- 39) J. Arviuex, Nucl. Phys. A **221** (1974), 253.
- 40) J. Chauvin and J. Arviuex, Nucl. Phys. A **247** (1975), 347.
- 41) L. D. Knutson, L. O. Lamm and J. E. McAninch, Phys. Rev. Lett. **71** (1993), 3762.
- 42) A. Kievsky, S. Rosati, W. Tornow and M. Viviani, Nucl. Phys. A **607** (1996), 402.
- 43) W. Tornow, A. Kievsky and H. Witała, Few-Body Systems **32** (2002), 53.
- 44) E. O. Alt, W. Sandhas and H. Ziegelmann, Phys. Rev. C **17** (1978), 1981.
- 45) G. H. Berthold, A. Stadler and H. Zankel, Phys. Rev. C **41** (1990), 1365.
- 46) R. B. Wiringa, V. G. J. Stoks and R. Schiavilla, Phys. Rev. C **51** (1995), 38.
- 47) B. S. Pudliner, V. R. Pandharipande, J. Carlson and R. B. Wiringa, Phys. Rev. Lett. **74** (1995), 4396.
- 48) A. J. Elwin, R. O. Lane and A. Langsdorf Jr., Phys. Rev. **128** (1962), 779.
- 49) D. C. Kocher and T. B. Clegg, Nucl. Phys. A **132** (1969), 455.
- 50) P. Schwarz, H. O. Klages, P. Doll, B. Haesner, J. Wilczynski, B. Zeitnitz and J. Kecskemeti, Nucl. Phys. A **398** (1983), 1.
- 51) K. Sagara, H. Oguri, S. Shimizu, K. Maeda, H. Nakamura, T. Nakashima and S. Morinobu, Phys. Rev. C **50** (1994), 576.
- 52) L. Schlessinger, Phys. Rev. **167** (1968), 1411.
- 53) J. L. Friar, D. Hüber and U. van Kolck, Phys. Rev. C **59** (1999), 53.
- 54) S. A. Coon and H. K. Han, Few-Body Systems **30** (2001), 131.
- 55) R. Machleidt, Adv. Nucl. Phys. **19** (1989), 189.
- 56) T. W. Phillips, B. L. Berman and J. D. Seagrave, Phys. Rev. C **22** (1980), 384.
- 57) J. M. Clement, P. Stoler, C. A. Goulding and R. W. Fairchild, Nucl. Phys. A **183** (1972), 51.
- 58) J. D. Seagrave and R. L. Hankel, Phys. Rev. **98** (1955), 666.
- 59) R. G. Nuckolls, C. L. Bailey, W. E. Bennett, T. Bergstrahl, H. T. Richards and J. H. Williams, Phys. Rev. **70** (1946), 805.
- 60) H. B. Willard, J. K. Bair and C. M. Jones, Phys. Lett. **9** (1964), 339.